Optofluidic FRET microlasers based on surface-supported liquid microdroplets

2014 Laser Phys. Lett. 11 045802

(http://iopscience.iop.org/1612-202X/11/4/045802)

IOP Publishing | Astro Ltd
Laser Physics Letters
Laser Phys. Lett. **11** (2014) 045802 (6pp)
doi:10.1088/1612-2011/11/4/045802

Letter

Optofluidic FRET microlasers based on surface-supported liquid microdroplets

E Özelci[1,3], M Aas[1,3], A Jonáš[2] and A Kiraz[1]

[1] Department of Physics, Koç University, Rumelifeneri Yolu, Sariyer, 34450 Istanbul, Turkey
[2] Department of Physics, Istanbul Technical University, Maslak, 34469 Istanbul, Turkey

E-mail: akiraz@ku.edu.tr

Received 16 January 2014
Accepted for publication 17 January 2014
Published 13 February 2014

Abstract

We demonstrate optofluidic microlasers using highly efficient non-radiative Förster resonance energy transfer (FRET) for pumping of gain medium placed within liquid microdroplets situated on a superhydrophobic surface. Microdroplets generated from a mixture of ethylene glycol, glycerol, and water and stained with the FRET donor–acceptor dye pair Rhodamine 6G-Rhodamine 700 serve as active optical resonant cavities hosting high-quality whispering gallery modes. Upon direct optical pumping of the donor with a pulsed laser, lasing is observed in the emission band of the acceptor as a result of efficient FRET coupling between the acceptor and donor molecules. FRET lasing is characterized for different acceptor and donor concentrations, and threshold pump fluences of acceptor lasing as low as 6.3 mJ cm^{-2} are demonstrated. We also verify the dominance of the non-radiative FRET over cavity-assisted radiative energy transfer for the range of parameters studied in the experiments.

Keywords: microcavity laser, microdroplet, FRET, superhydrophobic surface, whispering gallery mode

(Some figures may appear in colour only in the online journal)

1. Introduction

A ring resonator refers to a rotationally symmetric dielectric optical microcavity in which optical intensity can be confined in resonances called whispering gallery modes (WGMs). WGMs are morphology-dependent optical resonances that circulate near the rim of the cavity due to total internal reflection and enable light storage during relatively large periods of time thanks to their large quality factors (Q-factors) granted by the circular symmetry of the cavity. Ring resonators can be realized using various circularly symmetric geometries including microrings, microdisks, microcylinders, microspheres, and microtoroids [1] and they have distinct advantages as a photonic platform for applications in nonlinear optics [2, 3]. High Q-factor and small mode volume of the WGMs ensure observation of nonlinear optical phenomena such as dye lasing [4], stimulated Raman scattering [5], and Raman lasing [6] at relatively low threshold pump powers.

Optofluidic dye lasers developed using ring resonators hold great promise for biological and chemical sensing. Recently, lasers based on glass capillary ring resonators—also called optofluidic ring resonators (OFRRs)—have been used in conjunction with Förster resonance energy transfer (FRET) to achieve sensitive DNA detection [7]. In this demonstration, hybridization of the probe and target DNA molecules labeled with different dyes which served as FRET donor and acceptor pair led to the change in lasing color from the donor emission band to the acceptor emission band. In another recent demonstration, highly selective detection of single-nucleotide polymorphisms of DNA has been reported using OFRR and molecular beacon as a gain medium switchable by the analyte [8]. The presence of the target DNA ensured the operation

[3] EÖ and MA contributed equally to this work.

of the OFRR laser with pump power above lasing threshold. In contrast, with the same pump power, lasing was not observed and only negligible fluorescence background was detected when single-base mismatched DNA was added to the gain medium. This analog-to-digital detection scheme revealed an enhancement of over two orders of magnitude in the discrimination ratio between the target and single-base mismatched DNA compared to conventional fluorescence hybridization techniques. FRET lasing in an OFRR has also been used for highly sensitive fluorescent protein detection [9].

Optofluidic microcavities formed by liquid droplets represent alternative ring resonators that are suitable for such sensing applications. Due to their smooth surface and spherical shape determined by the tendency of liquids to minimize their interfacial area, microdroplets serve as natural optical cavities hosting high-Q WGMs [10–12]. In contrast to the OFRR where WGM–analyte interaction relies on evanescent mode coupling, in a microdroplet resonator, analytes may be placed directly inside the cavity. Thus, the analyte molecules that are located near the droplet surface interact with the peak WGM fields and stronger light–matter interactions can be achieved. These features make microdroplets ideally suited for sensing of biological species [13]. However, despite their potential, microdroplets have not been used in such applications to date. This has partly been due to the difficulties in handling microdroplets and integrating them with other microfluidic and optical components of the analytical system.

In this letter, we report FRET lasing in microdroplets located on a superhydrophobic surface. Deposition of droplets on superhydrophobic surfaces preserves their spherical shape while enabling position stabilization and easy coupling of light into and out of the droplets. Using glycerol/water microdroplets containing a single fluorescent dye, dye lasing was previously demonstrated in this geometry with direct optical pumping [14]. In the present work, we dope microdroplets composed of a mixture of water, ethylene glycol, and glycerol with donor and acceptor dye molecules that form a FRET pair. We first determine basic FRET characteristics of the chosen donor–acceptor pair in bulk solution. Subsequently, we study the spectral properties and pump threshold of lasing in surface-supported microdroplets containing donor and acceptor dyes. We provide experimental evidence for efficient pumping of laser emission of the acceptor molecules based on energy transfer and show that non-radiative FRET dominates over radiative cavity-enhanced energy coupling in the observed lasing spectra.

2. Experimental setup

Experimental setup employed in our FRET lasing studies was built around an inverted optical microscope, as described previously in [14]. Frequency-doubled 532 nm green beam output of a home-built, passively Q-switched Nd-YVO_4 laser (20 ns pulse width and 33 kHz repetition rate) was used for optical pumping of microdroplets. After being reflected from a dichroic mirror, the pump laser beam was sent through a water-immersion objective with high numerical aperture (Nikon 60×, NA = 1.2) and focused at the rim of fluorescently stained microdroplets deposited on a cover glass with superhydrophobic coating. A relatively large focal spot with 1.6 μm diameter was employed for the excitation beam in order to reduce sensitivity of the observed spectra to the precise position of the excitation beam with respect to the microdroplet. Fluorescence emission of microdroplets was collected by the same microscope objective, transmitted through the dichroic mirror, and dispersed by a monochromator (focal length 500 mm; Acton Research) on the chip of a cooled CCD detector (Pixis 100; Princeton Instruments). A shutter was added to the pump laser beam path to prevent fast photobleaching of the dye molecules in the microdroplets. This shutter was only opened during the spectrum acquisition time and provided a trigger signal for the CCD detector to synchronize the data recording. A polarizing beam splitter together with a half wave plate was used to control the green beam pump power. Microdroplets were imaged with an independent CCD camera placed at the other exit port of the microscope.

Superhydrophobic surfaces were prepared by spin coating hydrophobic silica nanoparticles (Aeroxide LE1; Degussa AG) dispersed in ethanol on cleaned microscope cover glasses [11]. These superhydrophobic surfaces are transparent to visible light and provide a high contact angle (>150°) for aqueous microdroplets [15]. To deposit micron-sized droplets on the surface, aerosols of the droplet liquid containing the dyes were generated using a compact ultrasonic nebulizer (JIH50, Beuer) and sprayed over the surface.

Rhodamine 6G (R6G; Sigma-Aldrich) and Rhodamine 700 (R700; Radiant Dyes) fluorescent dyes were selected as the FRET donor and acceptor molecules in our experiments. When dissolved in ethylene glycol (EG), R6G and R700 have their respective absorption peaks at 533 and 652 nm and respective emission peaks at 560 and 680 nm, thus providing a good spectral overlap for non-radiative energy transfer. R6G absorption profile is also well-suited for excitation with the green pump beam at 532 nm. For the systematic characterization of FRET efficiency and determination of Förster radius of the dye pair, selected dyes have to be soluble in the used droplet liquid up to the concentrations of 2 mM. In addition, generated droplets have to remain spherical and maintain a high contact angle during the experiment. In our first trials, we used pure EG as the solvent for R6G and R700. Since EG is less polar than glycerol and water, it was possible to prepare dye solutions with concentrations as high as 2.5 mM. At the same time, pure EG droplets still display initial contact angles higher than 140° on superhydrophobic surfaces. However, upon deposition of EG droplets on the surface, we observed that the droplets gradually wetted the surface and their contact angle decreased with time. This trend contrasted with the behavior of droplets of glycerol/water mixture that could preserve their high contact angles during prolonged periods of time. To increase the stability of the droplet contact angle, 35% w/w glycerol/water was added to EG in 1 to 9 volume ratio. Resulting droplets could then preserve their spherical geometry for periods of time that were significantly longer than those of pure EG droplets and they maintained contact angles between 150° and 160°, as determined by direct imaging of millimeter-sized droplets. Droplets prepared with

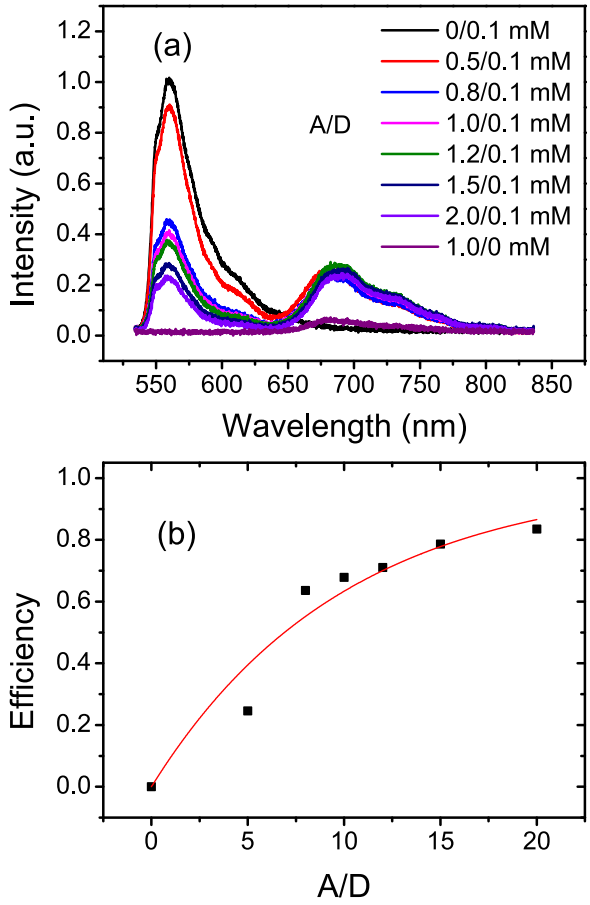

Figure 1. (a) Bulk fluorescence spectra recorded from solutions of R700/R6G dyes as an acceptor/donor pair in different concentration combinations A/D. All spectra were acquired with constant excitation by a 5 mW CW, 532 nm laser. The spectrum labeled 'A/D = 1.0/0 mM' was collected for 1.0 mM acceptor in the absence of donor and the other spectra were collected for a constant donor concentration of 0.1 mM and acceptor concentration changing from 0 to 2.0 mM. (b) Energy transfer efficiency between R6G and R700 dyes calculated from the spectra presented in part (a) and equation (1) (black squares). The red curve represents the fit of the experimental data points with equation (2).

this final mixture containing water, EG, and glycerol were observed to slowly evaporate during the experiments, as they were exposed to the ambient atmosphere with approximately 50% relative humidity. In order to minimize the uncertainty in dye concentrations caused by droplet evaporation, all the experiments reported in this letter were performed during approximately the first 10 min after the droplet generation. During this time, reduction of the droplet size was measured to be less than 7% which corresponds to the maximal increase of the dye concentrations of ∼20% with respect to the initial values. We note that all dye concentrations reported in this letter refer to those in the initial solutions used for droplet generation.

3. Results and discussions

To calculate the energy transfer efficiency and Förster radius of the R6G/R700 FRET pair, we recorded and analyzed emission spectra from bulk EG solutions with varying acceptor and donor concentrations (see figure 1). For these measurements, EG solutions of dyes were loaded into thin sample cells obtained by attaching two cover glasses to each other with double sided tape and fluorescence was excited by $\lambda = 532$ nm CW laser light with 5 mW output power. In figure 1(a), the solution of 1 mM R700 shows negligible emission in the absence of R6G because the pump wavelength is far away from the absorption band of R700. On the other hand, highest intensity of R6G emission is observed for the solution containing 0.1 mM R6G and no R700 in which FRET does not take place. As the R700 concentration is gradually increased in the presence of 0.1 mM R6G, the acceptor emission shows up with a peak around 690 nm and the donor intensity decreases due to the FRET mechanism. Figure 1(b) shows the energy transfer efficiency for each studied acceptor to donor ratio (A/D) obtained by

$$\eta = 1 - I_{\mathrm{D}}/I_{\mathrm{D}_0}, \tag{1}$$

where I_{D} and I_{D_0} are the donor emission intensity in the presence and absence of the acceptor, respectively. For each studied value of A/D, donor emission intensity was calculated by integrating the overall emission spectrum between 535 and 650 nm. According to [16], η can be described in terms of the acceptor concentration, c, by the following equation:

$$\eta = \exp(-1.42c/c_0), \tag{2}$$

where c_0 is a reference concentration which is called the critical transfer concentration. c_0 corresponds to an average of one acceptor molecule in a sphere of radius R_0, where the Förster radius R_0 is the critical distance for which non-radiative energy transfer rate from donor to acceptor and spontaneous emission rate of the donor are equal. The Förster radius can be found from c_0 by

$$R_0 = \left(\frac{3}{4\pi N c_0}\right)^{1/3}, \tag{3}$$

where N is the Avogadro number (6.023×10^{23} mol^{-1}) and c_0 is in units of M (mol l^{-1}). By fitting equation (2) to the experimental data of figure 1(b), we found $c_0 = (1.41 \pm 0.13)$ mM and $R_0 = (6.6 \pm 0.2)$ nm. For acceptor concentration of 0.69 mM, A/D = 6.9 and energy transfer efficiency becomes 50% which presents a highly efficient energy transfer between the donor and acceptor [17].

After characterizing the FRET properties of bulk R700/R6G solutions, we carried out experiments with R700/R6G stained EG/glycerol/water microdroplets standing on a superhydrophobic surface. Figure 2(a) demonstrates a series of FRET lasing spectra recorded from such droplets with a constant donor concentration of 0.1 mM and acceptor concentration varying between 0.5 and 2 mM. The droplets that were generated by the ultrasonic nebulizer had an initial large size distribution ranging from a few up to ∼50 μm in diameter. In our analysis we only considered droplets with diameters between 16 and 19 μm to minimize the uncertainty in the lasing properties caused by the microdroplet size variations. Similar to the bulk emission spectra of figure 1(a), the donor

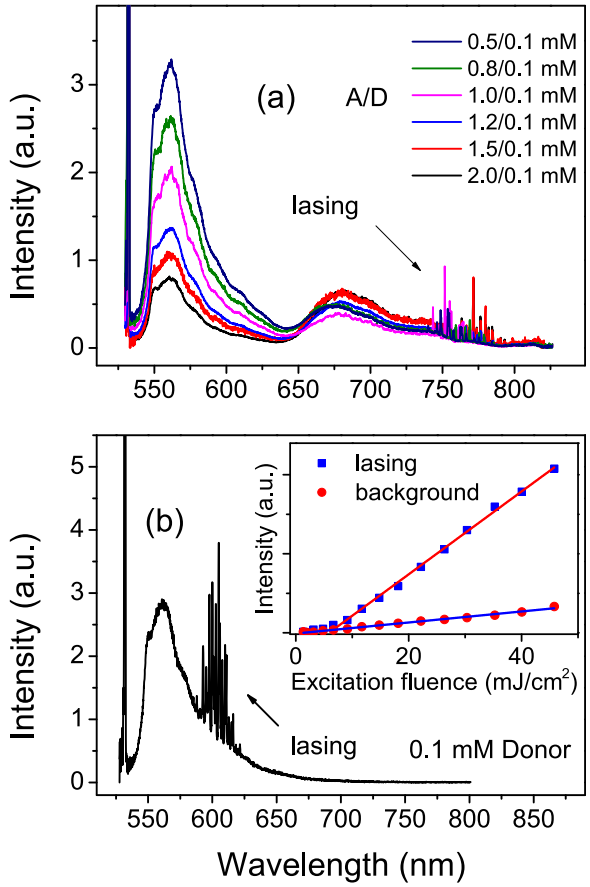

Figure 2. (a) FRET lasing spectra from R700/R6G stained microdroplets with diameters between 16 and 19 μm standing on a superhydrophobic surface. For all spectral recordings, excitation laser fluence was 74 mJ cm^{-2}. R6G concentration was kept constant at 0.1 mM and R700 concentration was varied from 0.5 to 2 mM. (b) Lasing in the donor emission region for a microdroplet containing 0.1 mM R6G and no R700 at 74 mJ cm^{-2} excitation laser fluence. Inset: determination of the pump threshold fluence from the dependence of the WGM emission intensity on the pump beam fluence.

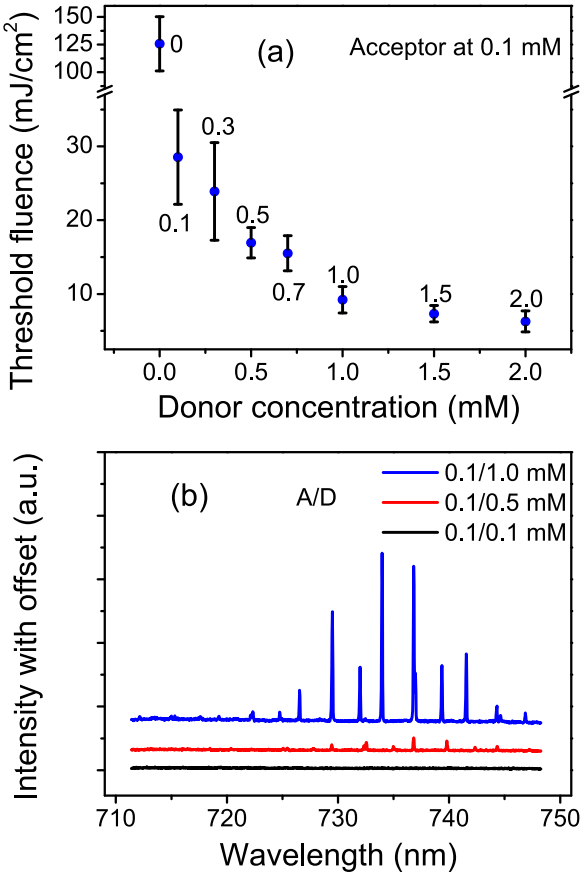

Figure 3. (a) Average threshold fluences of acceptor lasing for droplets with 16–19 μm diameter, constant acceptor concentration of 0.1 mM, and variable donor concentration from 0 to 2 mM. (b) Emission spectra in the acceptor lasing region recorded using excitation fluence of 16 mJ cm^{-2} for 18 μm diameter droplets doped with 0.1 mM R700 and 0.1, 0.5, and 1.0 mM R6G (bottom to top).

emission intensity in figure 2(a) decreases with increasing acceptor concentration but the corresponding changes in the background and lasing emission of the acceptor are negligible. In all of the spectra presented in figure 2(a), the excitation laser fluence was 74 mJ cm^{-2}. At this excitation fluence, lasing modes of droplets containing both dyes appear solely in the acceptor emission region between 740 and 800 nm. As shown in figure 2(b), in the absence of R700 acceptor dye, lasing from droplets containing 0.1 mM R6G is observed in the spectral region around 600 nm. Threshold analysis carried out as described in [14] and presented in the inset of figure 2(b) reveals threshold fluences around 7.3 mJ cm^{-2} for WGMs located in the donor emission region. Despite this low pump threshold for donor lasing from droplets that only contain R6G, donor lasing is completely suppressed due to the FRET mechanism when the acceptor is added at concentrations shown in figure 2(a) even at a high excitation fluence of 74 mJ cm^{-2}.

Another indication of the FRET lasing mechanism is provided by the analysis of threshold pump fluence of acceptor lasing for microdroplets with a constant acceptor and varying donor concentrations. In figure 3(a) we show the average pump threshold fluences of acceptor lasing for microdroplets with a constant acceptor concentration of 0.1 mM and donor concentration increasing from 0 to 2 mM. For each donor concentration, ten microdroplets with diameters between 16 and 19 μm were analyzed and the error bars indicate the standard deviation of threshold fluences of acceptor lasing determined from these ten measurements. Average lasing threshold fluence of the acceptor decreases from 126 mJ cm^{-2} for droplets with no donor to 6.3 mJ cm^{-2} for those containing donor at 2 mM concentration. In figure 3(b) emission spectra in the acceptor lasing region are shown for three droplets of similar size (~18 μm diameter) which were pumped using the same excitation fluence of 16 mJ cm^{-2}. These microdroplets have the same R700 concentration of 0.1 mM and different R6G concentrations of 0.1, 0.5, and 1.0 mM. For the droplet containing 0.1 mM R6G, acceptor lasing is not observed at the given pump laser fluence. For the droplet containing 0.5 mM R6G, acceptor lasing is observed with relatively low intensity as the pump fluence is only slightly above the lasing threshold for this particular donor concentration (see

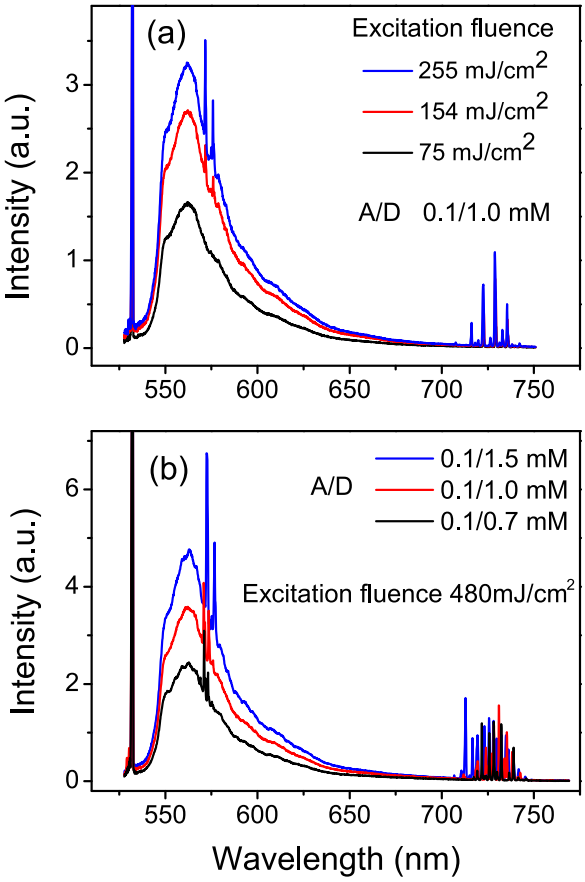

Figure 4. (a) Acceptor and donor lasing emission for a 19 μm diameter droplet with 0.1 mM R700 and 1.0 mM R6G excited with 75, 154, and 255 mJ cm^{-2} pump fluence. Threshold pump fluence for donor lasing was 132 mJ cm^{-2}. (b) Lasing emission spectra for three droplets with similar diameter (19 μm), identical acceptor concentration (0.1 mM) and pump fluence (480 mJ cm^{-2}), and different donor concentrations (0.7, 1.0, and 1.5 mM).

figure 3(a)). However, for the droplet with 1.0 mM R6G, intense acceptor lasing is visible as the pump fluence is well above the threshold fluence for the given dye concentrations.

In addition to the short-range energy transfer based on FRET, cavity-assisted radiative energy transfer through the WGMs can be observed in microdroplets [18, 19]. Cavity-assisted radiative energy transfer relies on long-time storage of photons emitted to WGMs by donor molecules, followed by their efficient re-absorption by acceptor molecules. To determine the dominant energy transfer mechanism in our case, we followed two sets of control experiments as previously reported by Shopova *et al* in [17]. In the first set of experiments, emission spectra from a single droplet exhibiting lasing in both donor and acceptor spectral regions were recorded with varied pump fluence. In figure 4(a) we show the lasing spectra recorded from a 19 μm diameter microdroplet with 0.1 mM acceptor and 1.0 mM donor concentrations at three different pump fluences. For this microdroplet, the threshold pump fluences for acceptor and donor lasing were determined as 9.3 mJ cm^{-2} and 132 mJ cm^{-2}, respectively. As illustrated by figure 4(a), when the pump fluence was consecutively set to 75, 154, and 255 mJ cm^{-2} i.e. below, near, and above the donor lasing threshold, the acceptor lasing peak intensities remained almost the same while the lasing peaks in the donor emission region emerged and grew. For the three given pump fluences, effective photon conversion efficiencies, γ, from the donor to the acceptor lasing were calculated by

$$\gamma = \left(1 + I_{\mathrm{D_{WGM}}}/I_{\mathrm{A_{WGM}}}\right)^{-1}, \qquad (4)$$

where $I_{\mathrm{D_{WGM}}}$ and $I_{\mathrm{A_{WGM}}}$ are the total intensities above the background level of the lasing WGMs in the donor and acceptor spectral regions, respectively. This calculation gave γ equal to 100, 81 and 66% for the shown spectra with the pump fluences that were 43% below, 16% above, and 92% above the donor lasing threshold, respectively. The decrease of γ with the increasing pump fluence indicates competition between non-radiative energy transfer from the donor to the acceptor and direct lasing emission from the donor that becomes dominant at high pump fluences. As argued by Shopova *et al* in [17], this provides evidence for ruling out radiative coupling between the donor and the acceptor molecules as in such a scenario, both donor and acceptor lasing intensity would increase with growing pump fluence.

In the second set of control experiments, we studied lasing in droplets of similar size ($\sim$19 μm), identical acceptor concentration (0.1 mM), identical pump fluence (480 mJ cm^{-2}), and different donor concentrations (0.7, 1.0, and 1.5 mM—see figure 4(b)). Under these experimental conditions, donor lasing intensity becomes stronger with increasing donor concentration and we would also expect higher acceptor lasing intensity if the dominant energy transfer mechanism was cavity-assisted radiative coupling. However, constant intensity of the acceptor lasing peaks together with decline in γ (76%, 68% and 62%) when the donor concentration increases (0.7, 1.0, and 1.5 mM) once again implies the dominance of the non-radiative FRET over the cavity-assisted radiative energy transfer. For the radiative energy transfer-dominated regime, γ is expected to be independent of the donor concentration, as reported in [18].

4. Summary

In summary, we have presented miniature optofluidic lasers that exploit surface-supported liquid microdroplets as optical resonant cavities and FRET for efficient pumping of the gain medium composed of two suitable fluorescent dyes that form FRET donor and acceptor pair. We showed that the lasing pump threshold can be effectively tuned by changing concentration of the donor and acceptor dyes in the droplet. We also verified that FRET is indeed the dominant mechanism of energy transfer within the composite gain medium. Demonstration of efficient FRET lasing in droplet-based resonators represents the first step towards applications of the droplet lasers in highly sensitive biological and chemical detection [20].

Acknowledgment

The authors would like to acknowledge financial support from TÜBİTAK (Grant No. 111T059).

References

[1] Vahala K J 2003 Optical microcavities *Nature* **424** 839

[2] Vollmer F and Arnold S 2008 Whispering-gallery-mode biosensing: label-free detection down to single molecules *Nature Methods* **5** 591–6

[3] Fan X and White I M 2011 Optofluidic microsystems for chemical and biological analysis *Nature Photon.* **5** 591–7

[4] Qian S-X, Snow J B, Tzeng H M and Chang R K 1986 Lasing droplets: highlighting the liquid-air interface by laser emission *Science* **231** 486

[5] Snow J B, Qian S-X and Chang R K 1985 Stimulated Raman scattering from individual water and ethanol droplets at morphology-dependent resonances *Opt. Lett.* **10** 37–9

[6] Sennaroglu A, Kiraz A, Dündar M A, Kurt A and Demirel A L 2007 Raman lasing near 630 nm from stationary glycerol-water microdroplets on a superhydrophobic surface *Opt. Lett.* **32** 2197–9

[7] Zhang X, Lee W and Fan X 2012 Bio-switchable optofluidic lasers based on DNA holliday junctions *Lab Chip* **12** 3673–5

[8] Sun Y and Fan X 2012 Distinguishing DNA by analog-to-digital-like conversion by using optofluidic lasers *Angew. Chem. Int. Ed. Engl.* **51** 1236–9

[9] Chen Q, Zhang X, Sun Y, Ritt M, Sivaramakrishnan S and Fan X 2013 Highly sensitive fluorescent protein fret detection using optofluidic lasers *Lab Chip* **13** 2679–81

[10] Ashkin A and Dziedzic J M 1977 Observation of resonances in the radiation pressure on dielectric spheres *Phys. Rev. Lett.* **38** 1351

[11] Kiraz A, Kurt A, Dündar M A and Demirel A L 2006 Simple largely tunable optical microcavity *Appl. Phys. Lett.* **89** 081118

[12] Datsyuk V V 2001 Optics of microdroplets *J. Mol. Liq.* **93** 159–75

[13] Vollmer F and Yang L 2012 Label-free detection with high-*q* microcavities: a review of biosensing mechanisms for integrated devices *Nanophotonics* **1** 267–91

[14] Kiraz A, Sennaroglu A, Doganay S, Dundar M A, Kurt A, Kalaycoglu H and Demirel A L 2007 Lasing from single, stationary, dye-doped glycerol/water microdroplets located on a superhydrophobic surface *Opt. Commun.* **276** 145–8

[15] Yüce M Y, Demirel A L and Menzel F 2005 Tuning the surface hydrophobicity of polymer/nanoparticle composite films in the wenzel regime by composition *Langmuir* **21** 5073

[16] Förster T 1959 Transfer mechanisms of electronic excitation *Discuss. Faraday Soc.* **27** 7–17

[17] Shopova S I, Cupps J M, Zhang P, Henderson E P, Lacey S and Fan X 2007 Opto-fluidic ring resonator lasers based on highly efficient resonant energy transfer *Opt. Express* **15** 12735–42

[18] Arnold S and Folan L M 1989 Energy transfer and the photon lifetime within an aerosol particle *Opt. Lett.* **14** 387–9

[19] Kiraz A, Doanay S, Kurt A and Demirel A L 2007 Enhanced energy transfer in single glycerol/water microdroplets standing on a superhydrophobic surface *Chem. Phys. Lett.* **444** 181–5

[20] White I M, Oveys H and Fan X 2006 Liquid-core optical ring-resonator sensors *Opt. Lett.* **31** 1319–21